Semiconductor Physics, Quantum Electronics & Optoelectronics, 2009. V. 12, N 1. P. 53-56.

PACS 73.40.Qv

Charge storage characteristics of gold nanoparticles embedded in alumina matrix

O. Bratus', A. Evtukh, E. Kaganovich, A. Kizjak, I. Kizjak, E. Manoilov
V. Lashkaryov Institute of Semiconductor Physics,
41, prospect Nauky, 03028 Kyiv, Ukraine

Abstract. The processes of charge accumulation in the nonvolatile memory metal-oxide-silicon capacitors with gold nanoparticles floating gate formed by the pulsed laser deposition method are investigated. The regularities of formation of alumina films with gold nanoparticles are the result of their deposition from the back flow of low-energy particles from the erosion torch. With removing from the torch axis, sizes of gold particles and the film thickness decreased. When recording the capacitance-voltage curves, the capture of a negative charge was observed. It was shown that the concentration of gold nanoparticles in alumina matrix and the thickness of nanocomposite films remarkably influenced on the stored charge. The observed flat band voltage shift was in the range 1 to 14 V. To explain the peculiarities of charge storage in the composite films, the electron transport through them was investigated.

Keywords: gold nanoparticle, alumina matrix, nanocomposite film, stored charge, electron transport.

Manuscript received 11.11.08; accepted for publication 18.12.08; published online 20.02.09.

1. Introduction

Memory-cell structures using nanoparticles as the charge storage media have received much attention as the promising candidates to replace the conventional dynamic random array memory or flash memories for future high speed and low power consumer memory devices. Metal nanoparticles memories, in comparison with their semiconductor counterparts, possess several advantages, namely: stronger coupling with the conduction channel, a wide range of available work functions, higher density of states around the Fermi level and smaller energy perturbation due to carrier confinement [1, 2]. The good memory effect is achieved, if the storage nodes are made of gold (Au) nanoparticles with the work function of 5.1 eV (effect of Pt (work function 5.32 eV) is better and of Ag (4.33 eV) is worse).

The introduction of high-*k* dielectric instead of the typical SiO_2 has brought improvement of programming efficiency and influenced on data retention. Thermally stable alumina (Al_2O_3) has the band gap of about 9 eV and dielectric constant ($\varepsilon_d \sim 9$) more than twice of that for SiO_2. It is considered as the promising candidate for gate dielectric.

Recently in the work [3], it was reported about the formation and charge storage characteristics of Au nanocrystals with the average diameter 5 nm embedded in amorphous Al_2O_3 matrix. Films were deposited using the pulsed laser deposition (PLD) method from the forward high-energy flow of erosion torch particles. The as-deposited films were subjected to post-annealing at 400 °C for 60 s in nitrogen ambient. Good performances in terms of large memory window were observed.

In this paper, we report also about the charge characteristics of the metal-insulator-semiconductor (MIS) structures with Al_2O_3 films containing Au nanoparticles obtained using PLD method. The purpose of this work is to investigate their characteristics in dependence on conditions of film deposition from the back flow of erosion torch low-energy particles without post-annealing.

2. Experiment

The pulsed laser deposition method was used to produce Au nanoparticles embedded into amorphous Al_2O_3 matrix. The Al+Au target was scanned with the beam of a YAG:Nd^{3+} laser emitting in the Q-switched mode at the wavelength $\lambda = 1.06$ μm. The repetition frequency and duration of the laser pulses were 25 Hz and 10 ns, respectively; the irradiation energy density was chosen in the range 2.5-20 J/cm^2. The films were formed by the particles from the reverse flux; monocrystalline silicon substrate was located in the plane of the target. The argon pressure was 10-20 Pa. The Au concentration was varied in the range 5-30 %. The deposition time was no longer than 30 min. The thickness of the films was from several tens to hundreds of nanometers.

To measure the current-voltage (*I-V*) and capacitance-voltage (*C-V*) curves, which characterize the electron transport and charge storage, respectively, the MIS structures with Au nanoparticles containing Al_2O_3 films as an insulator were formed on silicon substrate. The formation of MIS structures was completed by sputtering aluminium films on the frontal side through the mask and rearward surface. The ohmic Al contact with p-Si substrate was provided by thermal or laser annealing.

The *C-V* characteristics were measured with AMTs-1530 C meter at the testing signal frequency 1 MHz and voltage sweeping rate 50 mV/s within the range from –15 to +15 V. The *C-V* characteristic measurements proceeded from the voltage corresponding to depletion or inversion of the surface semiconductor layer (i.e., from positive gate voltages for the *p*-type semiconductor, from negative gate voltages for the n-type semiconductor) to those corresponding to accumulation and in the reverse direction. The high-frequency signal amplitude was 20 mV. The charging effect was determined from the shift of *C-V* characteristics at their measurements.

I-V characteristics were measured using a Keithley-6485 device. The voltage on upper metal electrode corresponds to accumulation conditions of semiconductor. It allows to exclude semiconductor influence when measuring the electron transport through composite films. Rebuilding *I-V* characteristics in various coordinates allowed us to clarify the current transport mechanism of charge carriers through nanocomposite films.

3. Results and discussion

The typical *C-V* characteristics of structures under investigation with Al_2O_3(Au) films obtained by PLD method are shown in Fig. 1. Clockwise hysteresis was observed indicating negative charging attributable to electron trapping from the metal electrode to the Au nanoparticles. The effective built-in charge changes the sign from negative to positive with growth of the Al_2O_3(Au) film thickness (Fig. 2).

An important peculiarity of the *C-V* characteristics is reduced capacitance under conditions of semiconductor surface accumulation (Fig. 1). This effect is caused by charging the nanoparticles at an increased gate voltage [4-6]. In the accumulation conditions, almost all the applied voltage drops inside the insulator. In this case, the electric field is high enough to promote electron tunneling from the gate on Au nanoparticles.

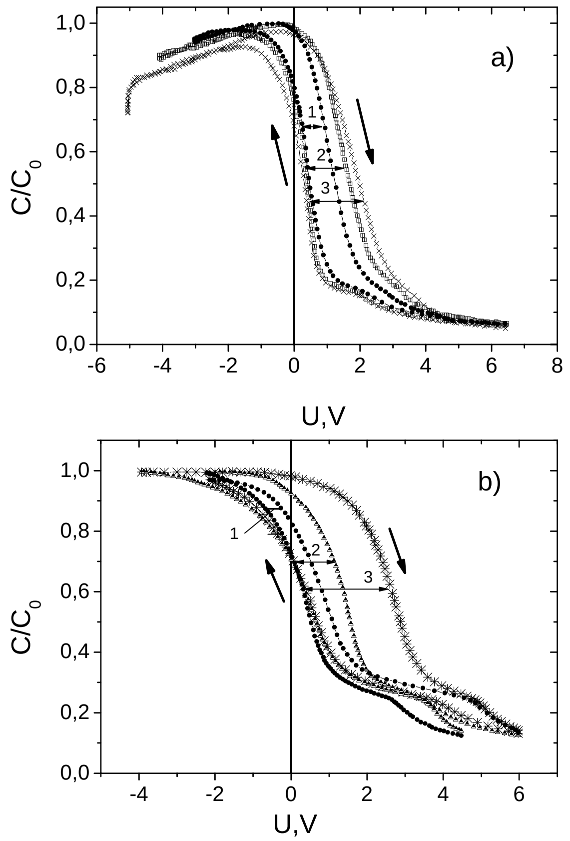

Fig. 1. Capacitance-voltage hysteresis after bidirectional sweeps of MIS structures with Al_2O_3(Au) film, concentration of Au particles in the film C_{Au}, %: a – 5, b – 30.

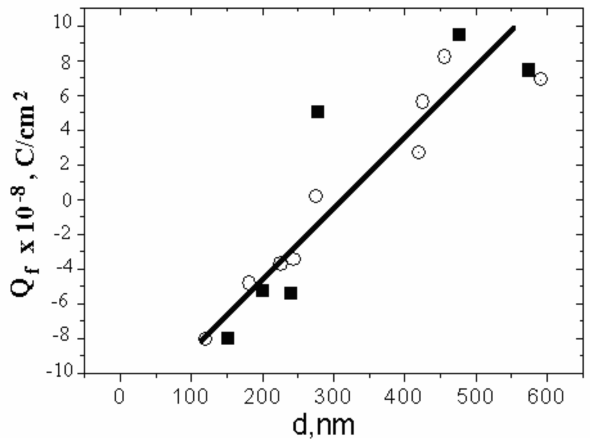

Fig. 2. Thickness dependence of the effective built-in charge in Al_2O_3(Au) film with C_{Au}, %: ○ – 5, ■ – 30.

The value and sign of the charge (ΔQ) captured in the insulator (Al_2O_3(Au)) of the MIS structure under the influence of electric field is determined from hysteresis of *C-V* characteristics when recording in two directions, from inversion to accumulation and vice versa, according to the following equation:

$$\Delta Q = C_{max} \times \Delta V_{FB}, \quad (1)$$

where ΔV_{FB} is the flat band voltage shift due to capture of the charge and C_{max} is the maximum capacitance under the accumulation conditions. The maximum value of the electric field in Al_2O_3(Au) films is reached under conditions of semiconductor surface accumulation. As a rule, positive values of the flat band voltage shift, ΔV_{FB}, are observed, evidencing the capture of effective negative charge in Au nanoparticles.

The dependences of ΔV_{FB} on maximum electric field in the films at *C-V* measurements with the film thickness as a parameter are shown in Fig. 3. As expected, the values of ΔV_{FB} increase with the increase of maximum electric fields. At a fixed electric field, the ΔV_{FB} grows with the thickness of the film. As can be seen, the higher Au content in the film (dashed lines in Fig. 3) causes the increase of the ΔV_{FB}. The thickness dependences of the captured charge ΔQ are shown in Fig. 4. The growth of the captured charge with film thickness is observed. The values of ΔQ are higher for the case of film with a higher content of Au particles.

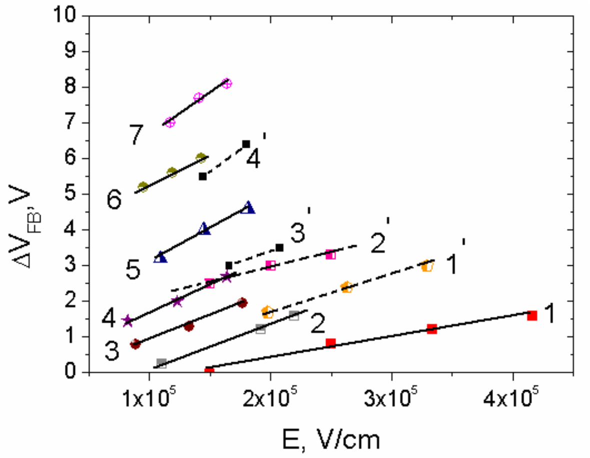

Fig. 3. Dependences of the flat band voltage shift on the maximum electric field for films with the thickness *d*, nm: *1* – 120, *2* – 182, *3* – 226, *4* – 244, *5* – 276, *6* – 420, *7* – 426 (C_{Au} = 5 %); *1′* – 152, *2′* – 200, *3′* – 241, *4′* – 278 (C_{Au} = 30 %).

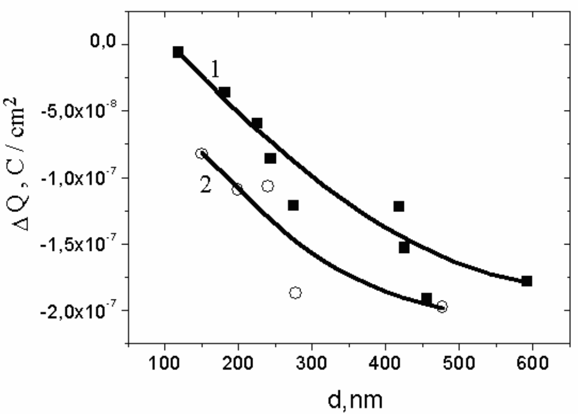

Fig. 4. Thickness dependences of the effective captured charge in Al_2O_3(Au) film with C_{Au}, %: *1* – 5, *2* – 30.

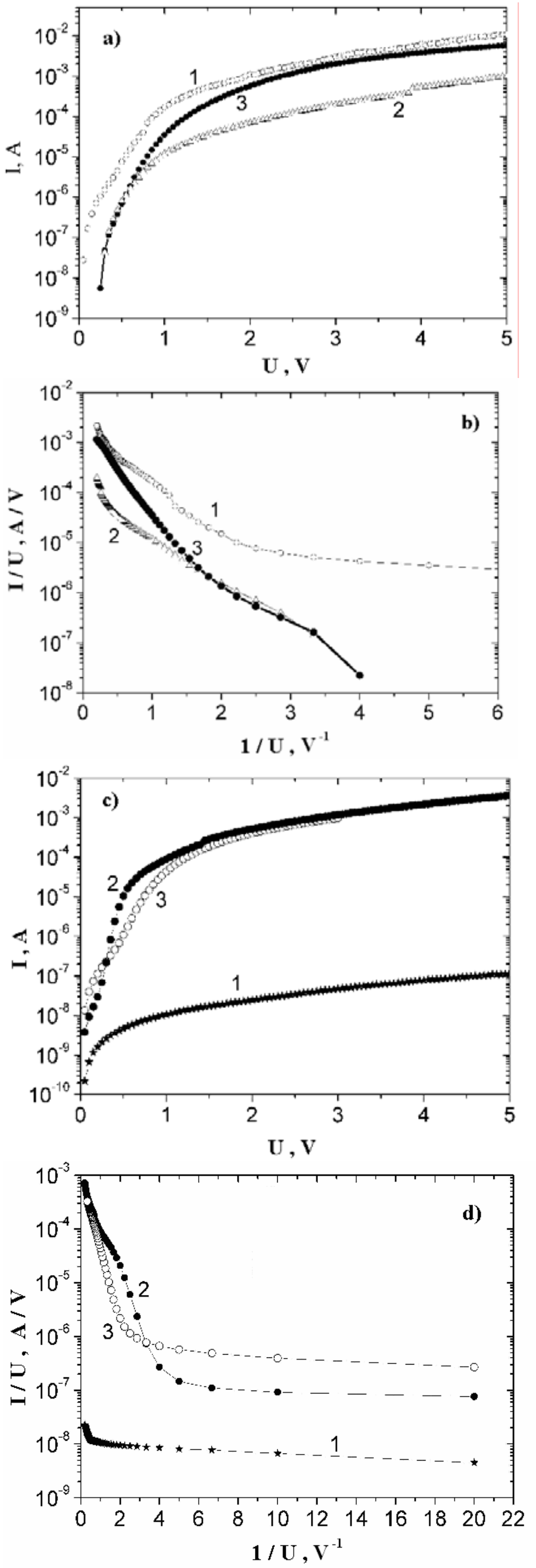

Fig. 5. *I-V* characteristics of nanocomposite Al_2O_3(Au) films before (a, b) and after (c, d) low temperature annealing (T = 450 °C, t = 30 min, N_2) with C_{Au}, %: *1,1′* – 0; *2,2′* – 5; *3,3′* – 30; b, d – in lg*I* /*U* ~ 1/*U* coordinates; C_{Au} is the Au content in films; $d_{Al_2O_3}$ = 60 nm.

Additional measurements were performed to clarify the sign and value of charge captured in nanocomposite Al_2O_3(Au) films and the charge carrier transport mechanism involved. The maximal value of negative voltage was varied at a fixed positive applied voltage and vice versa. Charge carriers (electrons) are captured mainly in Au nanoparticles embedded in the dielectric matrix. Some of them can be captured by traps in dielectrics and at Au nanoparticles / Al_2O_3 interfaces. Concentrations of localized energy states (traps) and delocalized energy states (states in the nanoparticles) do not restrict the charge carrier capture.

The typical *I-V* characteristics of the MIS structures with nanocomposite Al_2O_3(Au) films are shown in Fig. 5. The straightening of experimental *I-V* curves are observed in $\lg I/U \sim 1/U$ coordinates [7]. Rebuilding the *I-V* characteristics in various coordinates and analyzing them has allowed us to determine that carrier tunnelling through dielectric (Al_2O_3) layers between Au nanoparticles is the main current transport mechanism in high electric fields under forward bias (accumulation regime). The low temperature annealing at $T = 450$ °C during $t = 30$ min in N_2 didn't influence significantly on electrical conductivity of Au-containing films, while the annealing decreased significantly (some orders) the conductivity of the Al_2O_3 film without Au. In the case of Al_2O_3 film without Au, the electron transport is connected with a trap-assisted motion. It is possible to assume that the low temperature annealing in N_2 removes the electron traps from the bandgap of Al_2O_3 (passivates the broken bonds). The *I-V* characteristics of Al_2O_3(Au) with a lower content of Au (5 %) built in $\lg I/U \sim 1/U$ coordinates has two slopes, while for films with a high content of Au (30 %) there is only one slope. The slope of curves in $\lg I/U \sim 1/U$ coordinates is mainly determined by the energy barrier of Al_2O_3 dielectric layer between Au nanoparticles. In the case of low Au content, existence of two slopes and, as a result, of two different barrier heights can be caused by Au nanoparticles and Au traps.

4. Conclusions

The charge capture in MIS structure with nanocomposite Al_2O_3(Au) films obtained by the pulse laser deposition method was investigated. The main peculiarities of charge storage were determined, namely: (i) effective built-in charge changed sign from negative to positive with film thickness growth; (ii) the negative charge was captured in the films; (iii) the storage of negative charge was increased with growth of Al_2O_3(Au) film thickness, electric field and Au content in the films. *I-V* characteristics were straightened in $\lg I/U \sim 1/U$ coordinates. It is indicative of carrier tunnelling through Al_2O_3 layers between Au nanoparticles as a main current transport mechanism in high electric fields.

References

1. Z. Liu, C. Lee, V. Narayanan, G. Pei, E.C. Kan, Metal nanocrystal memories. I. Device design and fabrication // *IEEE Trans. Electron Dev.* **49**(9), p. 1606-1613 (2002).
2. P.H. Yeh, L.J. Chen, P.T. Liu, D.Y. Wang, T.C. Chang, Metal nanocrystals as charge storage nodes for non-volatile memory devices // *Electrochemica Acta* **52**, p. 2920-2926 (2007).
3. C.L. Yuan, P.S. Lee, S.L. Ye, Formation, photoluminescence and charge storage characteristics of Au nanocrystals embedded in amorphous Al_2O_3 matrix // *EPL* **80,** p. 67003 (2007).
4. Y. Liu, T.P. Chen, C.Y. Ng, M.S. Tse, S. Fung, Y.C. Liu, S. Li, P. Zhao, Charging effect on electrical characteristics of MOS structures with Si nanocrystals distribution in gate oxide // *Electrochem. Solid-State Lett.* **7**(7)**,** G134-G137 (2004).
5. Y. Liu, T.P. Chen, C.Y. Ng, M.S. Tse, S. Fung, A.A. Tseng, Influence of Si nanocrystal distribution in the oxide on the charging behavior of MOS structures // *IEEE Trans. Electron Dev.* **53**(4), p. 914-917 (2006).
6. O.L. Bratus', A.A. Evtukh, V.A. Ievtukh, V.G. Litovchenko, Nanocomposite SiO_2(Si) films as a medium for non-volatile memory // *J. Non-Crystal. Solids* **354,** p. 4278-4281 (2008).
7. B. Abeles, P. Sheng, M.D. Coutts, Y. Arie, Structural and electrical properties of granular metal films // *Adv. Phys.* **24**(3), p. 407-461 (1975).